

Synthesis and Characterization of Holmium Based Metal-Organic Frameworks

Muhammad Abbas ¹, Murtaza Degani ¹, Simin Sheybani ¹, Tejas Shah ¹, Monu Joy ¹, and Kenneth J. Balkus Jr. ^{1,*}

¹Department of Chemistry and Biochemistry, The University of Texas at Dallas, 800 West Campbell Rd, Richardson, TX 75080, United States

*Correspondence: Kenneth J. Balkus Jr, email: balkus@utdallas.edu

Single crystal X-ray diffraction (SC-XRD)

Single crystal X-ray diffraction data for both compounds was collected on a Bruker D8-QUEST X-ray diffractometer equipped with a Mo μ S microfocus X-ray source ($\lambda = 0.71073 \text{ \AA}$) and a PHOTON II CPAD detector. The measurement was performed at 200 K using an Oxford Cryosystems low-temperature device. The APEX-IV software suite was used for data collection, cell refinement, and data reduction. Absorption corrections were applied using SADABS.¹ Space group assignments were determined by examination of systematic absences, E-statistics, and successive refinement of the structures. The structure was solved with dual-space method using SHELXT² and refined against $|F|^2$ on all data by full-matrix least squares with SHELXL.³ All non-hydrogen atoms were refined with anisotropic displacement parameters. The C-H atoms were positioned with idealized geometry and were refined with fixed isotropic displacement parameters [$U_{\text{eq}}(\text{H}) = -1.2U_{\text{eq}}(\text{C}), -1.5U_{\text{eq}}(\text{C})$ for $-\text{CH}_3$] using a riding model. CCDC 2356198–2356199 contains the supplementary crystallographic data for this paper. These data can be obtained free of charge from the Cambridge Crystallographic Data Centre via www.ccdc.cam.ac.uk. Selected crystal data and details on structure determinations are listed in Table S1.

X-ray Photoelectron Spectroscopy (XPS)

X-ray photoelectron spectra were collected on a PHI VersaProbe II Scanning XPS Microprobe (Physical Electronics Inc, Chanhassen, Minnesota) equipped with Al K α X-ray source ($E_p = 1486.7$ eV) at a pressure 1.6×10^{-9} Torr. The high-resolution spectra were collected at the pass energy of 23.5 eV with a step size of 0.2 eV. Photoelectron spectra were obtained using a charge compensation of 2 μ A. The sample surface was cleaned by sputtering Gas-Cluster Ion Beam (GCIB) with an energy of 5 kV and cluster size of ~ 2500 argon atoms. The data was processed with software CasaXPS and binding energies were doubly calibrated to adventitious C $_{1s}$ at 284.8 eV and Au 4f $_{7/2}$ at 83.95 eV.

Powder X-ray diffraction (PXRD)

PXRD patterns were collected on an Ultima IV X-ray diffractometer (Rigaku) equipped with Cu K α radiation, with a scan rate of 2 $^\circ$ /min and a step size of 0.04 $^\circ$. The simulated XRD patterns were generated from the CIF files using a crystal structure visualization tool Mercury⁹ (Cambridge Crystallographic Data Centre).

Gas Adsorption Analysis and Sample Preparation

The adsorption/desorption isotherms were obtained on ASAP 2020 Plus (Micromeritics instrument corporation) at 77 K for N $_2$ and 273 K for CO $_2$. For the surface area and porosity analysis, MOFs crystals were washed 3 times with fresh DMF and activated at 170 $^\circ$ C under vacuum. The surface area was calculated by built-in Brunauer–Emmett–Teller (BET) model. Ultra-high purity CO $_2$ and N $_2$ were used for the analysis.

The scanning electron microscopy (SEM) and Energy Dispersive X-ray Spectroscopy (EDX)

SEM and EDX was performed on a Zeiss EVO LS SEM and an Aztec Instruments Oxford EDX

Thermogravimetric analysis (TGA)

Thermogravimetric analysis was conducted using a SDT Q600 (TA Instruments). The samples were then heated from room temperature to 700 °C at a rate of 10 °C/min under air with a flow rate of 20 mL/min.

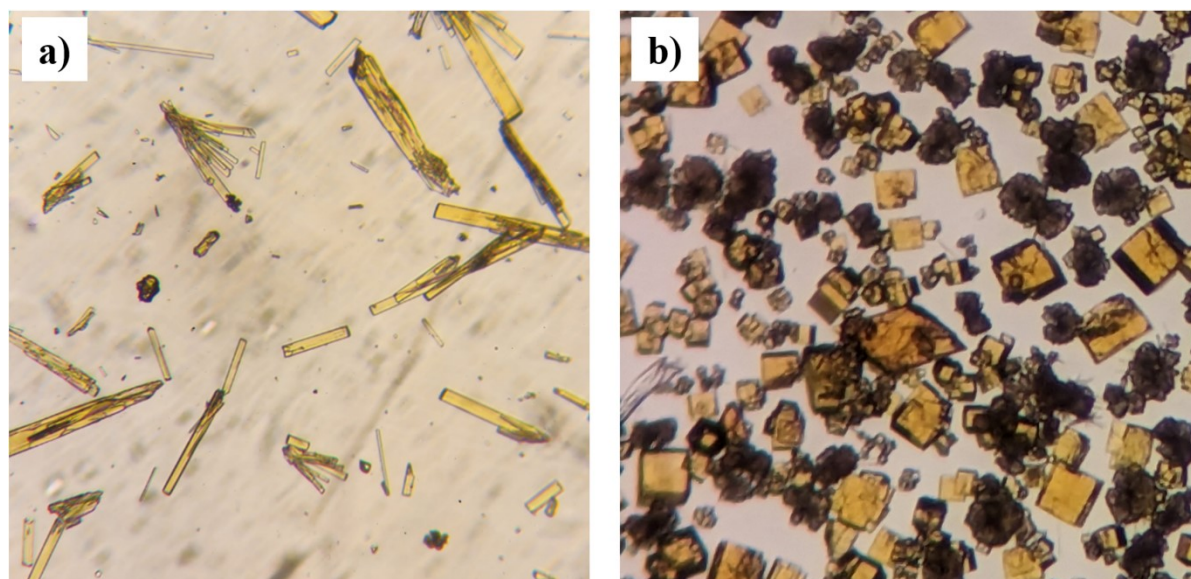


Figure S1. Optical Images of crystals of the (a) Ho_2 -abtc and (b) Ho_6 -abtc.

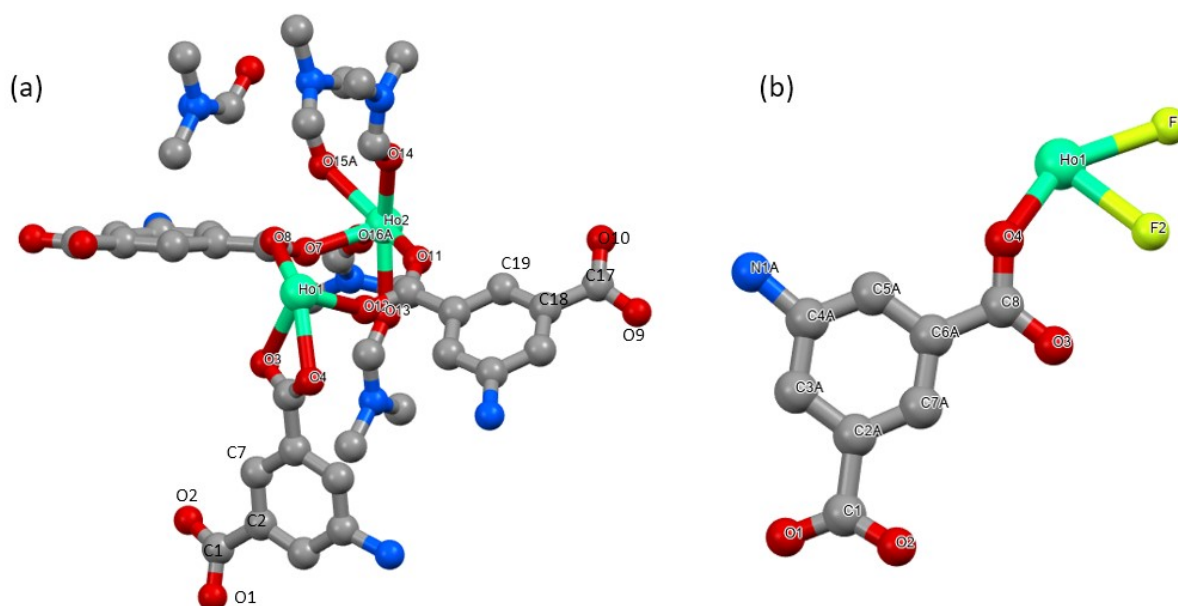


Figure S2. Asymmetric units of (a) Ho_2 -abtc and (b) Ho_6 -abtc.

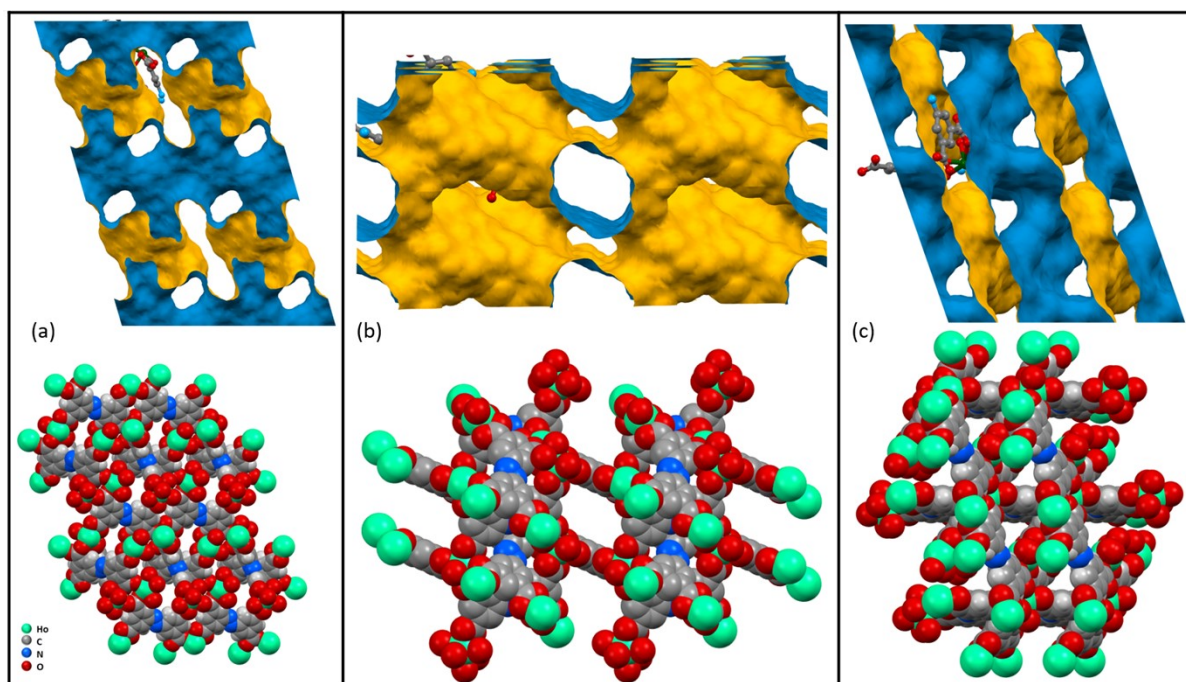


Figure S3. Solvent accessible surface and corresponding channels of the Ho_2 -abtc along the a , b , and c -axis (outer surface = yellow, inner surface = blue).

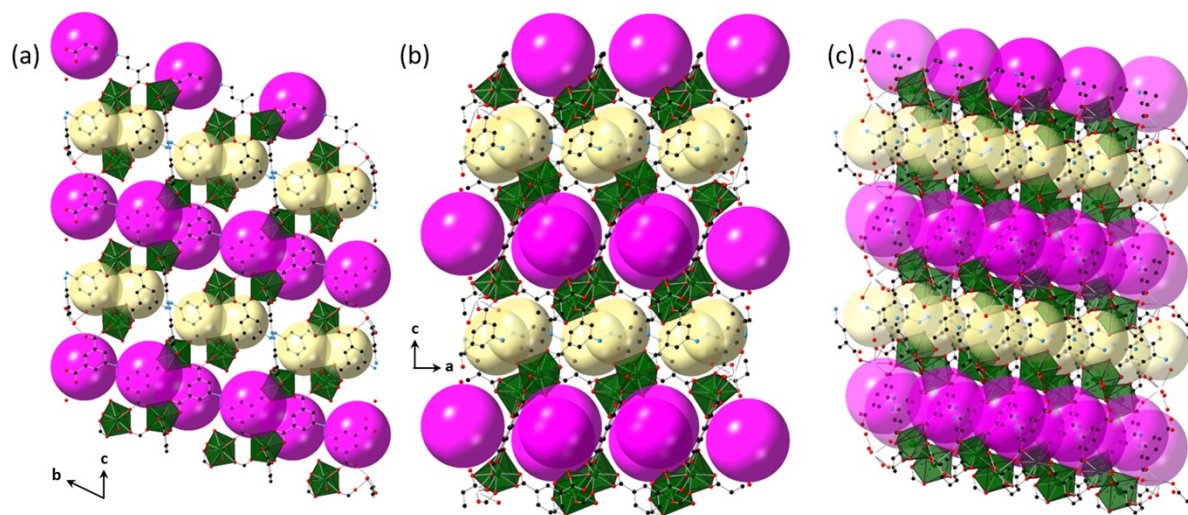


Figure S4. Crystal structure packing of the Ho_2 -abtc along the a , b , and $[100]$ directions.

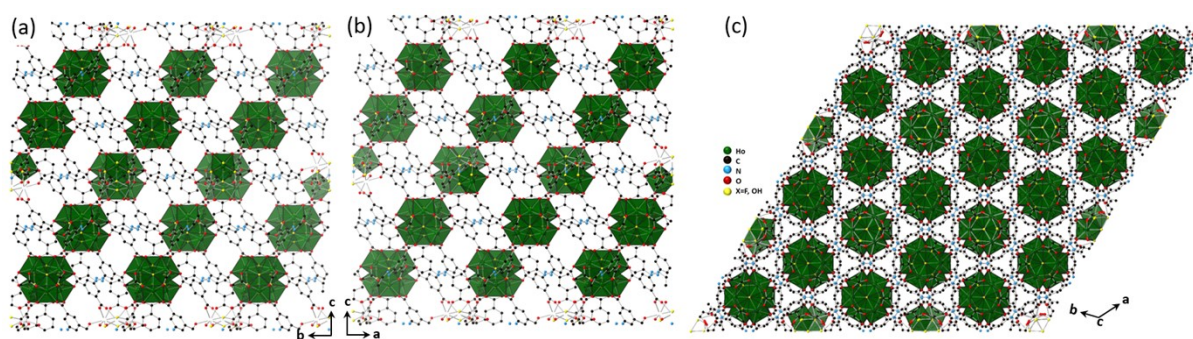


Figure S5. Crystal structure packing of the $\text{Ho}_6\text{-abtc}$ along the a , b , and c axes.

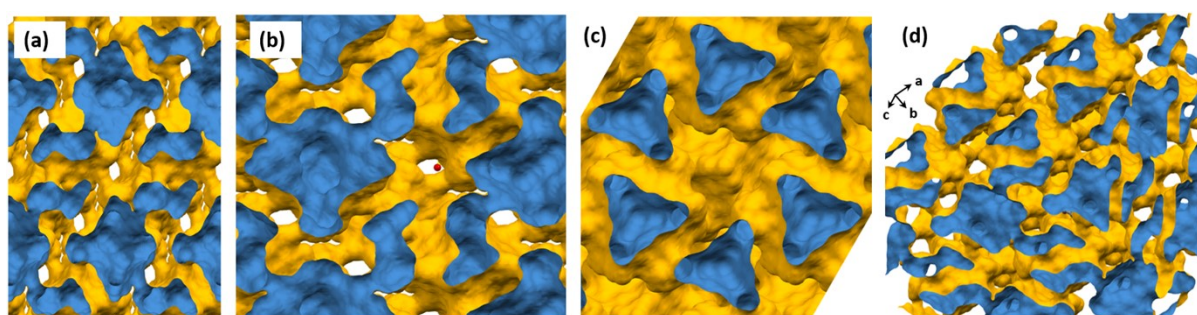


Figure S6.. Solvent accessible surface of the $\text{Ho}_6\text{-abtc}$ along the a , b , and c -axis (outer surface = yellow, inner surface = blue).

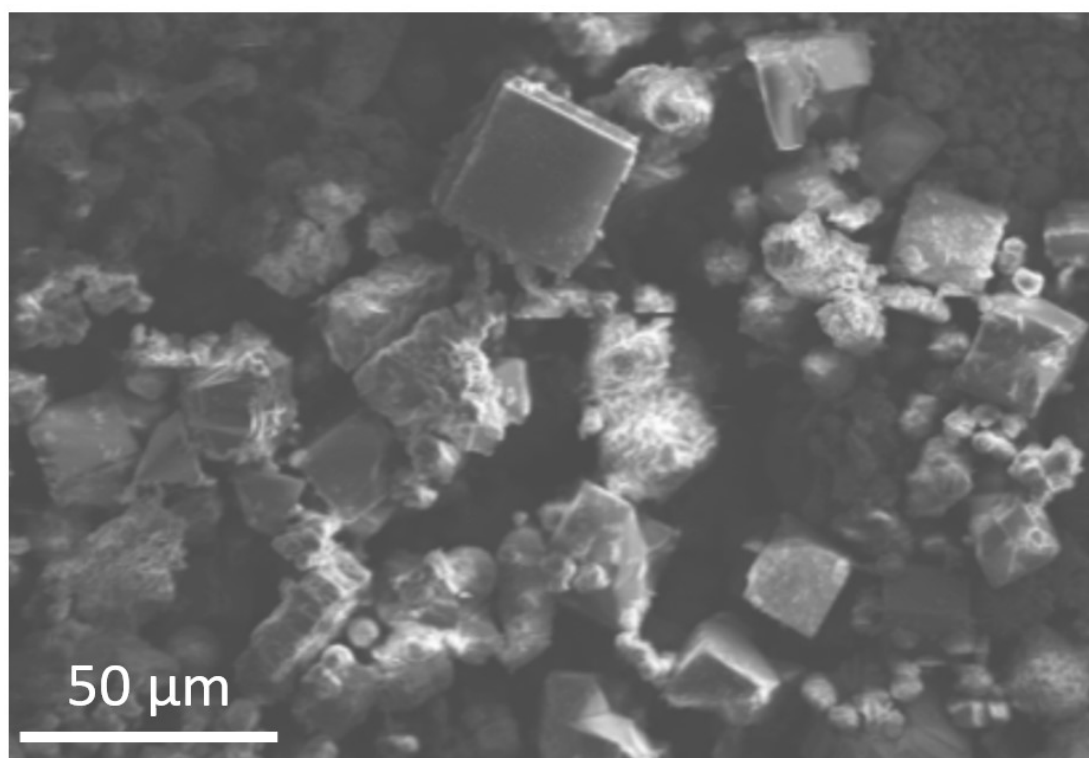


Figure S7. SEM image of the $\text{Ho}_6\text{-abtc}$.

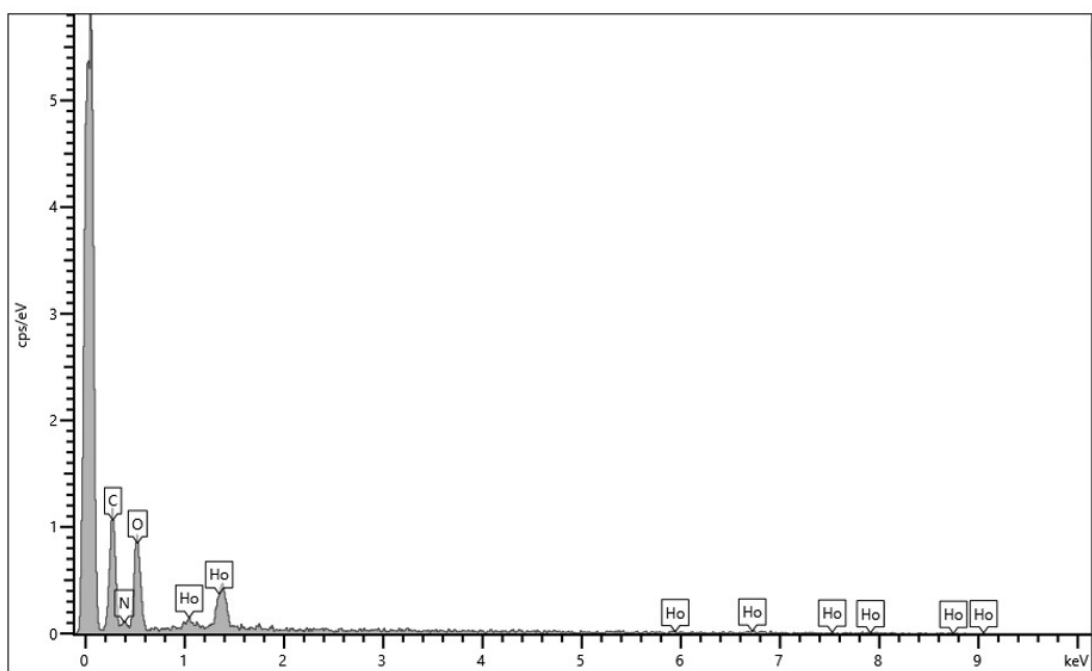


Figure S8. EDS spectrum of the Ho_2-abtc .

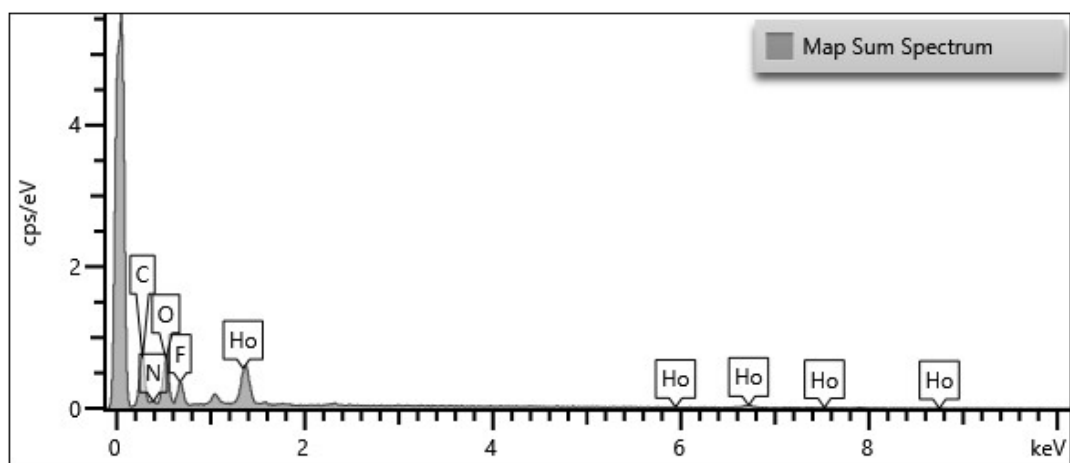


Figure S9. EDS spectrum of the Ho_6-abtc .

Table S1. EDS map sum spectrum of the Ho₂-abtc.

Element	Line Type	Apparent Concentration	k Ratio	Wt%	Wt% Sigma	Standard Label
C	K series	0.04	0.00037	42.63	6.63	C Vit
N	K series	0.02	0.00003	7.68	2.88	BN
O	K series	0.04	0.00015	25.49	4.05	SiO ₂
Ho	L series	0.02	0.00018	24.20	11.40	Ho (v)
Total:				100.00		

Table S2. EDS map sum spectrum of the Ho₆-abtc.

Element	Line Type	Apparent Concentration	k Ratio	Wt%	Wt% Sigma	Standard Label
C	K series	0.02	0.00023	25.7	1.89	C Vit
N	K series	0.01	0.00002	3.2	0.73	BN
O	K series	0.03	0.00011	12.90	0.94	SiO ₂
F	K series	0.03	0.00006	4.4	0.52	CaF ₂
Ho	L series	0.05	0.00054	53.8	3.30	Ho (v)
Total:				100.00		

Table S3. Percent composition of Ho₆-abtc calculated from the survey XPS spectrum.

Element	RSF	FWHM	Raw Area	Atomic%	Weight%
Ho 4d	13.35	10.10	76613.79	6.53	46.84
C 1s	1.0	4.22	60098.46	68.32	35.69
N 1s	1.8	2.82	4579.76	2.89	1.76
O 1s	2.93	4.28	52955.87	20.50	14.26
F 1s	4.43	4.07	6869.70	1.76	1.45

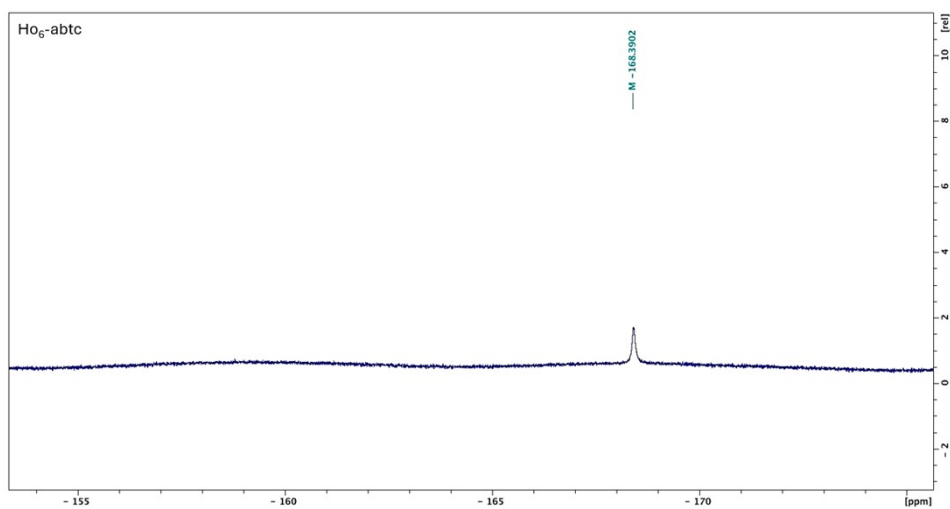


Figure S10. The ^{19}F -NMR spectra of the acid digested $\text{Ho}_6\text{-abtc}$ MOF exhibiting a peak at -168.39 for HF.

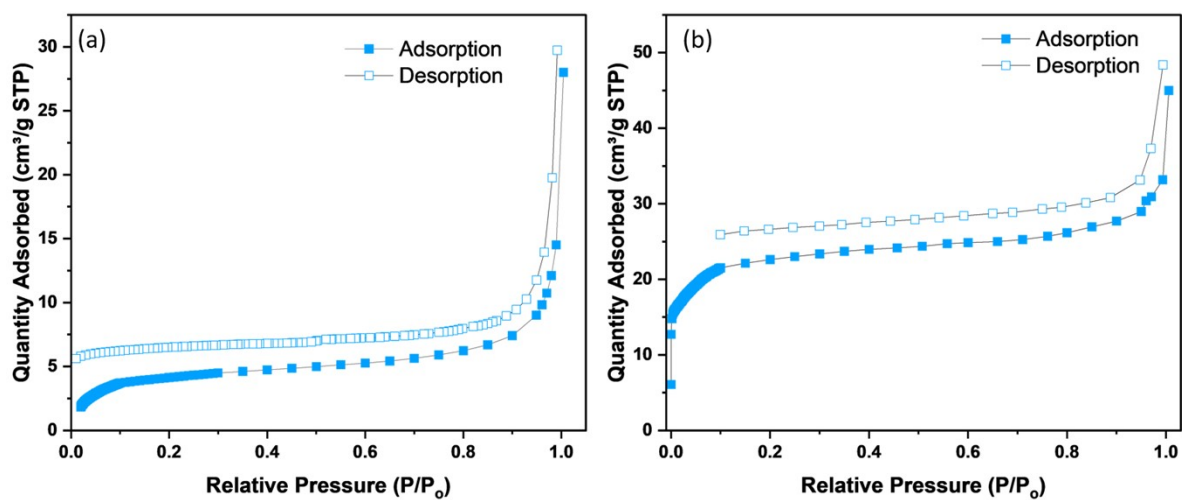


Figure S11. Nitrogen adsorption-desorption isotherms at 77 K for (a) $\text{Ho}_2\text{-abtc}$ and (b) $\text{Ho}_6\text{-abtc}$.

References

1. Bruker (2001) SADABS Bruker AXS Inc., Madison, Wisconsin, USA
2. G. M. Sheldrick, Acta Cryst A **2015**, 71, 3–8.
3. G. M. Sheldrick, Acta Cryst C **2015**, 71, 3–8.